NANO LETTERS

Letter

pubs.acs.org/NanoLett

Large-Angle, Multifunctional Metagratings Based on Freeform Multimode Geometries

David Sell,[†] Jianji Yang,[‡] Sage Doshay,[†] Rui Yang,[‡] and Jonathan A. Fan*[,‡]

[†]Department of Applied Physics and [‡]Department of Electrical Engineering, Stanford University, Stanford, California 94305, United States

Supporting Information

ABSTRACT: We show that silicon-based metagratings capable of large-angle, multifunctional performance can be realized using inverse freeform design. These devices consist of nonintuitive nanoscale patterns and support a large number of spatially overlapping optical modes per unit area. The quantity of modes, in combination with their optimized responses, provides the degrees of freedom required to produce high-efficiency devices. To demonstrate the power and versatility of our approach, we fabricate metagratings that can efficiently deflect light to 75° angles and multifunctional devices that can steer beams to different diffraction orders based on wavelength. A theoretical analysis of the Bloch modes supported by these devices elucidates the spatial mode profiles and coupling dynamics that make high-performance beam deflection possible. This approach represents a new paradigm in nano-optical mode engineering and utilizes different physics from the current state-of-the-art, which is based on the stitching of noninteracting waveguide structures. We envision that inverse design will enable new classes of high-performance photonic systems and new strategies toward the nanoscale control of light fields.

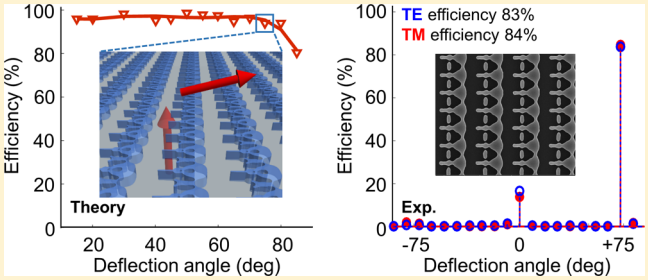

KEYWORDS: *Metasurfaces, metamaterials, blazed grating, Bloch mode, multimode, large-angle deflection, multifunction*

Metasurfaces[1] serve as nanoscale-phased arrays and have broad utility in spectroscopy,[2] integrated optics,[3] optical filtering,[4] and holography.[5] These devices employ concepts in subwavelength-scale engineering to produce custom phase profile responses, and current state-of-the-art devices employ building blocks with physically intuitive optical responses. Among the earliest examples were metagratings consisting of a series of titanium dioxide pillars, which cumulatively produced an effective medium supporting a blazed refractive index profile[6,7] More recently, silicon nanowaveguides were used as building blocks in transmit arrays,[8] and optical response based on geometric phase was specified using collections of anisotropic waveguides.[9,10] In nearly all of these conceptualizations, individual nanowaveguides are stitched together with sufficient spacing to minimize coupling between adjacent elements to produce a phase profile response. High efficiencies are possible in these transmissive devices because they utilize dielectric materials with negligible absorption.

For relatively small deflection angles, echelle gratings and periodic nanowaveguide-based metasurfaces, that is, metagratings, can steer light into a single diffraction order with high efficiency. Metagratings in this operation regime have large periods, and multiple nanowaveguide elements can be stitched within a single period to sufficiently sample a linear phase profile response. These concepts have generalized to metasurface lenses that possess numeric apertures as large as 0.8,[10] which enables the collection of light within an angular span of 0−50°. However, at larger bending angles, echelle gratings and nanowaveguide-based metadevices exhibit strongly reduced efficiency (Figure 1a). For echelle gratings, this is due to physical shadowing effects that arise from the sawtooth geometry itself. For metagratings, this is due in part to the limited number of waveguide elements that can fit within the width of a grating period. We will examine the ramifications of this limit later. This inaccessibility to large bending angles hinders the creation of large-angle gratings for spectroscopy and also lenses with large numeric apertures, which are critically important for high-performance imaging applications such as those in molecular microscopy.[11]

We propose an entirely different strategy for metagrating design using adjoint-based topology optimization. With this approach, we produce devices that possess nonintuitive layouts (Figure 1b) and support large numbers of spatially overlapping nano-optical modes. As such, these devices utilize different physical principles compared to those based on decoupled nanowaveguides. This new paradigm in nano-optical mode engineering enables deflection efficiencies that far exceed the current state-of-the-art for large angles (Figure 1a). In this study, we demonstrate metagratings that can deflect light to angles as large as 80°. We also show how our design

Received: March 14, 2017
Revised: April 28, 2017
Published: May 1, 2017

DOI: 10.1021/acs.nanolett.7b01082
Nano Lett. 2017, 17, 3752−3757

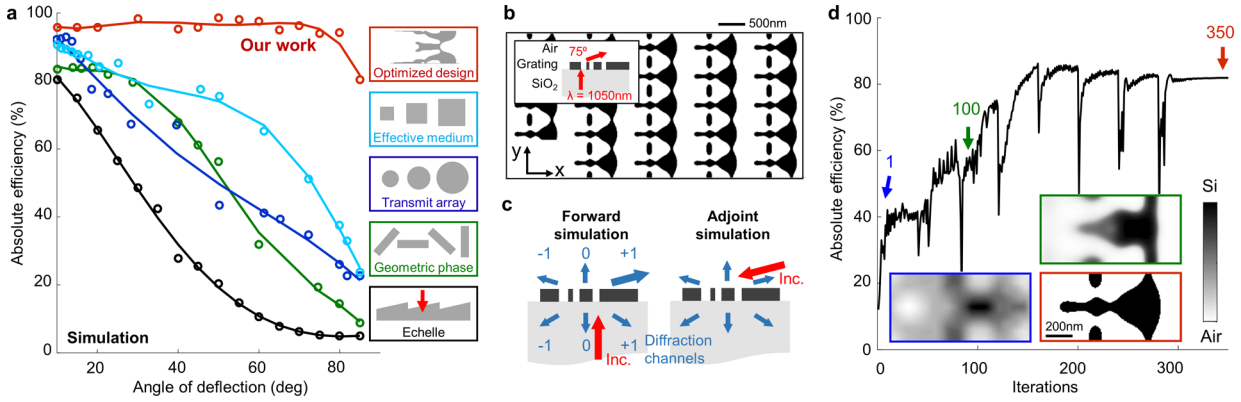

Figure 1. Overview of metagrating design using topology optimization. (a) Simulated deflection efficiencies of various transmission grating types as a function of deflection angle. These include the classical echelle grating, three types of established metagrating designs, and our topology-optimized metagrating. These devices deflect normally incident TE- and TM-polarized light at a single wavelength, and the plotted points represent the deflection efficiency averaged over both polarizations. The wavelengths and materials used in these simulations are listed in Table S1. (b) Top view of a 75° deflection metagrating designed using topology optimization. The device deflects normally incident TE- and TM-polarized light at a wavelength of 1050 nm. Black represents silicon and white represents air. (c) Schematic of the forward and adjoint simulations used to optimize a large-angle transmissive metagrating, which deflects normally incident light into the (+1, 0) diffraction channel. Also sketched are the five other diffraction channels in the system. (d) Plot of deflection efficiency over the course of the topology optimization process for the metagrating in (b). A total of 350 iterations are used to design the device. The sharp dips represent a strong geometric blur that is applied every 40 iterations to eliminate small features (see Supporting Information). The insets show the dielectric constant distribution in a single unit cell of the metagrating at different stages of the optimization process.

methodology can generalize to multifunctional metasurfaces, and we demonstrate a high-efficiency wavelength splitter.

Our method for designing transmissive metagratings that deflect a normally incident plane wave with a specific polarization and wavelength is summarized as follows. The initial design consists of a random dielectric continuum, with values ranging between the dielectric constants of air and silicon. To improve the figure of merit (FoM), which corresponds to deflection efficiency, an iterative process is performed that uses two electromagnetic simulations per iteration, a forward and an adjoint simulation (Figure 1c). These simulations produce two sets of electromagnetic field profiles within the device, which serve to specify changes in the dielectric constant at every location in a manner that improves the FoM. Over the course of multiple iterations, the dielectric continuum in the device converges to the dielectric constant of either silicon or air (Figure 1d). Importantly, our optimization method can readily extend to multiple input polarizations and wavelengths by performing forward and adjoint simulations for each optical degree of freedom per iteration. The details of our methodology are in the Supporting Information and other sources.[12,13]

We note that a variety of optimization techniques, including topology optimization, have previously been explored in nanophotonic device design. One subset involves heuristic optimization schemes such as binary search, particle swarm, and evolutionary optimization algorithms.[14−21] These schemes can apply to devices containing relatively simple geometries, but they become computationally expensive and have limited efficacy with more intricate devices. The application of topology optimization to more complex nanophotonic devices originates from silicon photonic devices by the Sigmund group,[22,23] and it has since been applied to other on-chip photonic devices,[24] photonic crystals,[25] and plasmonic absorbers.[26] Boundary optimization has been utilized to realize semiconducting absorbers[27] and optical sorters based on scalar diffraction.[28] To the best of our knowledge, high-performance metadevices have not been previously realized using inverse design.

Our metagratings consist of a distributed and deeply subwavelength array of touching and nearly connected silicon nanostructures. The interconnected and complex structures operate with qualitatively different physics than nanowave-guide-based designs. We explore the underlying operating principles of our large-angle metagratings by examining their optical modes. Metagratings consisting of a single thin film with vertically etched features can be generally treated as a vertically oriented Fabry−Perot cavity supporting a set of Bloch modes. The substrate−grating and grating−air interfaces serve as the cavity mirrors. The plane wave incident on the metagrating excites these modes, which bounce within the cavity. Whenever a mode interacts with a cavity mirror, a combination of three processes can occur, as described by coupled mode analysis (Figure 2a).[29,30] First, the mode can reflect from the interface. Second, the mode can interact with and exchange energy with other modes. Third, the mode can scatter out of the cavity into several discrete diffraction channels (six channels are shown in the example in Figure 2a). As such, each diffraction channel contains contributions from all of the modes. High deflection efficiency in the desired diffraction channel is achieved when the out-coupled plane waves from all the Bloch modes in that channel strongly constructively interfere (Figure 2a, dashed boxes).

As a representative example, we analyze the Bloch modes for the transmissive 75° metagrating featured in Figure 1b, for transverse magnetic (TM)-polarized incident light. An analysis for transverse electric (TE)-polarized incident light is presented in the Supporting Information. The mode profiles are extracted from our rigorous coupled-wave analysis (RCWA) solver.[31] This device supports eight propagating Bloch modes, which have effective modal refractive indices ranging from air-like to silicon-like. The device also supports many evanescent modes, which have decay lengths that are much shorter than the device thickness and therefore couple minimally with the diffraction channels. The intricate field profiles of the propagating modes

DOI: 10.1021/acs.nanolett.7b01082
Nano Lett. 2017, 17, 3752−3757

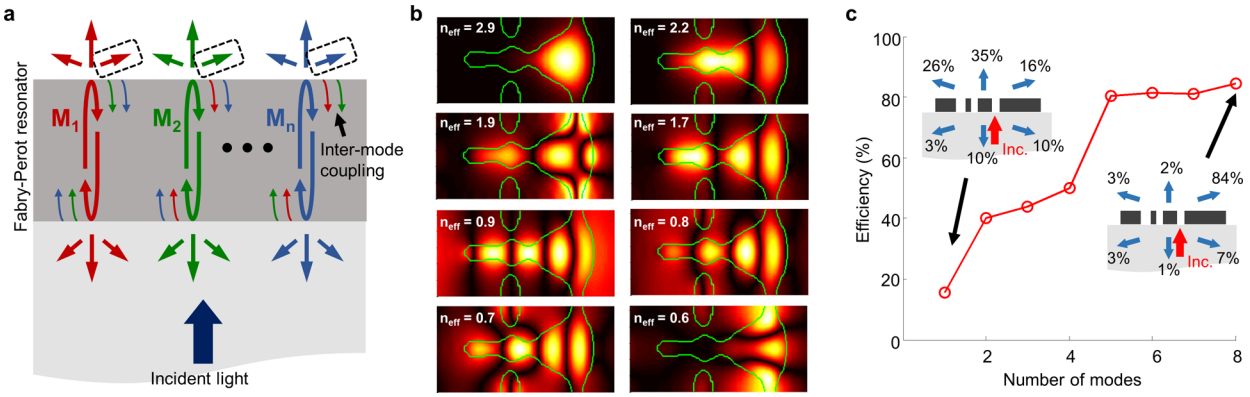

Figure 2. Theoretical metagrating mode analysis. (a) Schematic of mode dynamics in a metagrating device, as described by coupled Bloch mode analysis. The Bloch modes, labeled $\mathbf{M}_1$ to $\mathbf{M}_n$, bounce within the metagrating. When these modes scatter at an interface, they can reflect (thick curved arrows), couple with other modes (thin curved arrows), and couple into diffraction channels (thick straight arrows). Strong beam deflection occurs when there is strong constructive interference between out-coupled modes in the desired diffraction channel (dashed boxes). (b) $|\mathbf{H}|$ profiles of the modes supported by the metagrating designed in Figure 1b. The normally incident beam is TM-polarized. The effective mode refractive indices n_{eff} are indicated, and outlines of the silicon structure are drawn in green. (c) Plot of deflection efficiency as a function of number of modes included in the calculation, using the modes in (b). When only the $n_{\text{eff}} = 2.9$ mode is included (i.e., number of modes = 1), only 16% of the light is deflected into the desired grating order (inset, top left). As more modes are included (added in order of decreasing n_{eff}), the deflection efficiency of the metagrating gradually increases. When all eight modes are included, the deflection efficiency into the desired channel is 84% (inset, bottom right).

are plotted in Figure 2b. Each of the modes possesses some degree of spatial overlap with each of the other modes, which enables the possibility of energy exchange between modes at the cavity mirror interface. A quantitative analysis of each mode indicates that no individual mode couples efficiently into the desired diffraction channel. However, the constructive interference of all eight out-coupled modes in the desired diffraction channel yields high deflection efficiency (Figure 2c).

This example is indicative of the many factors in device design that need to be controlled to enable efficient large-angle deflection. First, the effective refractive index and spatial profile of each mode need to be tailored such that the modes constructively interfere as they couple into the desired diffraction channel. Second, the coupling strengths of the incident plane wave into the modes; the modes into the diffraction channels; and the modes with other modes need to be properly tuned. These coupling parameters involve both the propagating and evanescent Bloch modes, which together specify the electromagnetic field boundary conditions at the metagrating interfaces. Third, it is intuitively helpful for the metagrating to support as many total modes as possible, which allows the potential for more degrees of freedom in the design to be tailored to better fit the parameters above. This design problem is complex and ultimately intractable to address using physically intuitive design procedures. Our optimization method addresses many of the posed difficulties and specifies the spatial profiles of the propagating and evanescent modes in an automated fashion to enable highly efficient beam steering.

To compare our analysis with the existing state-of-the-art, we perform a benchmark analysis of a transmissive 75° metagrating designed using the effective medium approach. An individual grating period has space for only two nanopillars, and the device supports only three propagating Bloch modes. Two of the modes show strong field localization within an individual nanopillar (Figure S8), which is consistent with the design methodology of stitching together individual waveguide elements. The third mode has a low effective refractive index, and its fields are predominantly in the air region of the grating. Due in part to the relatively small number of modes and nonoptimized spatial mode profiles, the grating efficiency is low.

We fabricate and characterize topology-optimized metagrating structures operating at near-infrared wavelengths. Our initial substrate is a silicon dioxide wafer on which we grow a layer of polycrystalline silicon by chemical vapor deposition. We then pattern 200 μm diameter circular grating devices using electron beam lithography, followed by reactive ion etching. The devices are optically characterized using a weakly focused tunable white light laser as our input source, and we detect the diffracted light beams using a germanium detector mounted on a goniometer. Further experimental details are in Section 1 in the Supporting Information.

To reduce device sensitivity to fabrication imperfections, we incorporate robustness algorithms[32] into our design process. These algorithms explicitly include the effects of geometric dilation and erosion in each iteration of the optimization process, with the goal of reducing the impact of geometric variability on device efficiency (see Supporting Information). This incorporation of robustness into the device design necessitates a trade-off with optimal device efficiency. Devices that possess higher overall performance at the expense of being less robust can be experimentally realized with more precise fabrication.

We first characterize the 75° transmission grating from Figure 1b, which is designed to deflect normally-incident TE waves (E-field component along the y-axis, see Figure 1b for the coordinate system) and TM waves (H-field component along y-axis) with a wavelength of 1050 nm within the $x-z$ plane. These devices do not diffract light within the $y-z$ plane because the grating period along the y-axis is subwavelength in scale. A scanning electron microscopy (SEM) image of the device is presented in Figure 3a, and the silicon nanostructures have morphologies that match well with the theoretical design. Tilted SEM images of the device (Figure S10) show vertical sidewalls, indicative of high-quality silicon etching. For our analysis, we characterize both the absolute and relative efficiencies of the device. Absolute efficiency refers to the power in the deflected light beam normalized to the power of

DOI: 10.1021/acs.nanolett.7b01082
Nano Lett. 2017, 17, 3752−3757

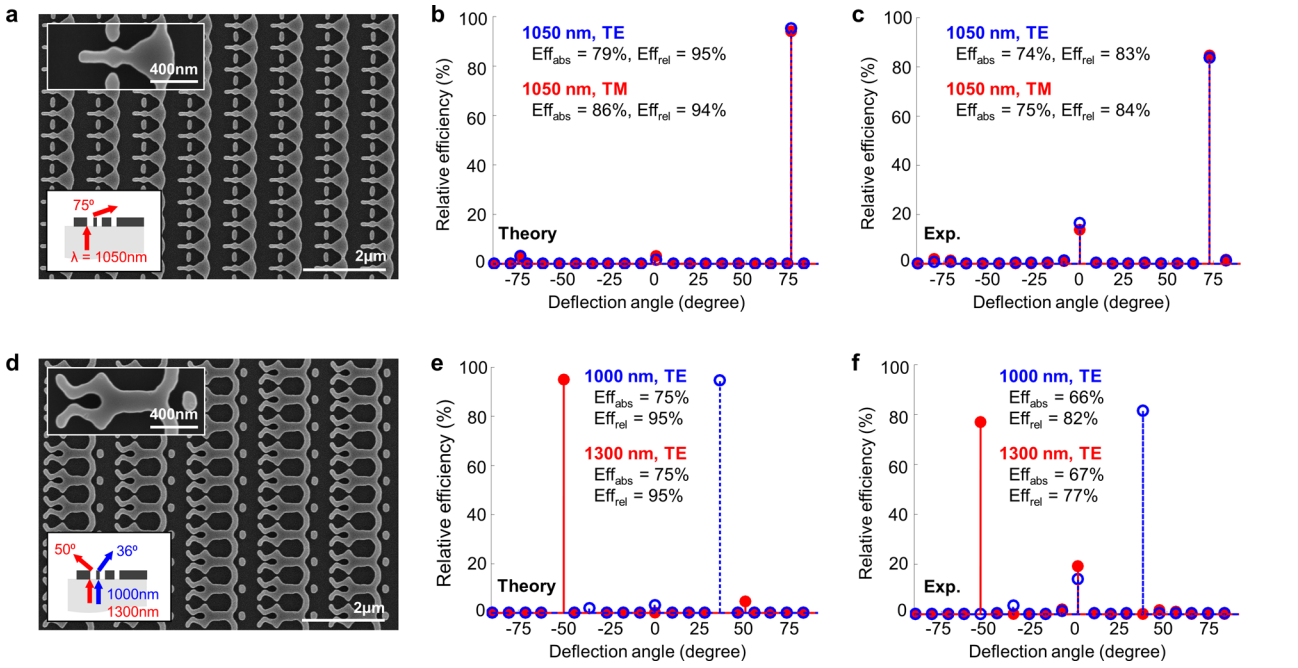

Figure 3. Experimental characterization of metagrating devices. Scanning electron microscopy image of (a) the 75° beam deflector shown in Figure 1b, and (d) a wavelength splitter for normally incident TE-polarized light. Top insets: magnified image of an individual metagrating unit cell. Bottom insets: schematic of the metagrating function. (b) Theoretical and (c) experimental deflection efficiencies of the beam deflector. Data points are plotted separately for TE- and TM-polarized incidence and are normalized as relative efficiencies. (e) Theoretical and (f) experimental deflection efficiencies of the wavelength splitter. Data points are plotted separately for 1000 and 1300 nm incident wavelengths and are normalized as relative efficiencies. In all plots, values for absolute and relative efficiency are specified.

light transmitted through a bare silicon dioxide substrate. Relative efficiency refers to the power in the deflected light beam normalized to the total power transmitted through the device.

Theoretical and experimental deflection efficiencies are summarized in Figure 3b and 3c, respectively. The experimental data show that the device operates with high absolute and relative efficiencies. The absolute deflection efficiencies for TE- and TM-polarized light are measured to be 74% and 75%, respectively, which are close to the theoretical values. The numerical accuracy of the theoretical values, calculated using our RCWA solver, is benchmarked in the Supporting Information and has less than ∼1% error. The relative efficiencies for TE- and TM-polarized light are both above 80%, indicating strong preferential coupling to the (+1, 0) diffraction channel compared to the (−1, 0) and (0, 0) diffraction channels. The discrepancies between the experimental and theoretical efficiencies are due in part to minor geometric imperfections in the fabricated device. Overall, the device displays experimental efficiencies that are significantly higher than the theoretical efficiencies of the current state-of-the-art (Figure 1a).

Our design methodology can readily generalize to high-efficiency, multifunctional devices. We define an individual function to be the deflection of an incident beam with a particular wavelength and polarization into a specific diffraction channel. As a proof of concept, we design, fabricate, and characterize a metagrating that deflects 1000 nm TE-polarized light to a +36° angle ((+1, 0) diffraction channel) and 1300 nm TE-polarized light to a −50° angle ((−1, 0) diffraction channel). Each of these desired functions are incorporated in a straightforward fashion into our iterative metagrating design procedure by performing forward and adjoint simulations for each function in each iteration. This design objective would be difficult and even intractable to achieve using physically intuitive design principles. SEM images and efficiency plots of our device are displayed in Figure 3d–f and show that high-efficiency wavelength splitters can be theoretically designed and experimentally realized. The absolute deflection efficiencies at the two target wavelengths are above 60% and are within 10% of their theoretical values. The relative efficiencies at these wavelengths are near 80%. For each wavelength, deflection into the desired diffraction order is over 20× more efficient compared to deflection into the opposite diffraction order.

In summary, we utilize concepts in inverse freeform design to construct large-angle silicon metagrating deflectors that display theoretical and experimental efficiencies that far exceed the current state-of-the-art. We also show that these design principles can readily extend to multifunctional devices. These devices represent a new class of high-performance metasurfaces that operate based on spatially overlapping optical modes, each possessing nonintuitive spatial mode profiles and intricate mode interaction dynamics. We envision that these concepts in optical mode engineering, enabled by iterative optimization solvers, will extend to the design of aperiodic, multiwavelength, multifunctional metasurfaces with performances that operate near the limits of composite nanomaterials engineering.

■ ASSOCIATED CONTENT

Supporting Information

The Supporting Information is available free of charge on the ACS Publications website at DOI: 10.1021/acs.nanolett.7b01082.

Details of the fabrication steps, experimental setup, adjoint-based optimization and coupled Bloch mode

DOI: 10.1021/acs.nanolett.7b01082
Nano Lett. 2017, 17, 3752−3757

theory, mode analysis of conventional and topology-optimized deflectors, and geometric parameters of the metagratings from Figure 1a (PDF)
Movie showing the topology optimization of a deflector (AVI)

AUTHOR INFORMATION

Corresponding Author

*E-mail: jonfan@stanford.edu.

ORCID

Jianji Yang: 0000-0003-3903-5094
Jonathan A. Fan: 0000-0001-9816-9979

Author Contributions

J.F. supervised the study. D.S. and J.Y. performed the simulations. D.S., S.D., and R.Y. performed the experiments. All authors contributed to experimental planning, data analysis, and writing the paper.

Notes

The authors declare no competing financial interest.

ACKNOWLEDGMENTS

The samples in this study were fabricated at the Stanford Nanofabrication Facility and Stanford Nano Shared Facility. The simulations were performed in the Sherlock computing cluster at Stanford University. This work was supported by the U.S. Air Force under Award Number FA9550-15-1-0161, the Office of Naval Research under Award Number N00014-16-1-2630, and the Alfred P. Sloan Foundation. D.S. was supported by the National Science Foundation (NSF) through the NSF Graduate Research Fellowship, and S.D. was supported by the Department of Defense through the National Defense Science and Engineering Graduate Fellowship Program. J.Y. asnd D.S. acknowledge J.-P. Hugonin for assistance on numerical simulations.

REFERENCES

(1) Genevet, P.; Capasso, F.; Aieta, F.; Khorasaninejad, M.; Devlin, R. Recent advances in planar optics: from plasmonic to dielectric metasurfaces. *Optica* **2017**, *4*, 139−152.
(2) Pors, A.; Nielsen, M. G.; Bozhevolnyi, S. I. Plasmonic metagratings for simultaneous determination of Stokes parameters. *Optica* **2015**, *2*, 716−723.
(3) Taillaert, D.; Van Laere, F.; Ayre, M.; Bogaerts, W.; Van Thourhout, D.; Bienstman, P.; Baets, R. Grating Couplers for Coupling between Optical Fibers and Nanophotonic Waveguides. *Jpn. J. Appl. Phys.* **2006**, *45*, 6071.
(4) Chang-Hasnain, C. J.; Yang, W. High-contrast gratings for integrated optoelectronics. *Adv. Opt. Photonics* **2012**, *4*, 379−440.
(5) Genevet, P.; Capasso, F. Holographic optical metasurfaces: a review of current progress. *Rep. Prog. Phys.* **2015**, *78*, 024401.
(6) Lalanne, P.; Astilean, S.; Chavel, P.; Cambril, E.; Launois, H. Blazed binary subwavelength gratings with efficiencies larger than those of conventional échelette gratings. *Opt. Lett.* **1998**, *23*, 1081−1083.
(7) Lalanne, P.; Astilean, S.; Chavel, P.; Cambril, E.; Launois, H. Design and fabrication of blazed binary diffractive elements with sampling periods smaller than the structural cutoff. *J. Opt. Soc. Am. A* **1999**, *16*, 1143−1156.
(8) Arbabi, A.; Horie, Y.; Bagheri, M.; Faraon, A. Dielectric metasurfaces for complete control of phase and polarization with subwavelength spatial resolution and high transmission. *Nat. Nanotechnol.* **2015**, *10*, 937−943.
(9) Lin, D.; Fan, P.; Hasman, E.; Brongersma, M. L. Dielectric gradient metasurface optical elements. *Science* **2014**, *345*, 298−302.
(10) Khorasaninejad, M.; Chen, W. T.; Devlin, R. C.; Oh, J.; Zhu, A. Y.; Capasso, F. Metalenses at visible wavelengths: Diffraction-limited focusing and subwavelength resolution imaging. *Science* **2016**, *352*, 1190−1194.
(11) Lee, K. G.; Chen, X. W.; Eghlidi, H.; Kukura, P.; Lettow, R.; Renn, A.; Sandoghdar, V.; Gotzinger, S. A planar dielectric antenna for directional single-photon emission and near-unity collection efficiency. *Nat. Photonics* **2011**, *5*, 166−169.
(12) Bendsoe, M. P.; Sigmund, O. *Topology Optimization: Theory, Methods, and Applications*; Springer: Berlin Heidelberg, 2003
(13) Lalau-Keraly, C. M.; Bhargava, S.; Miller, O. D.; Yablonovitch, E. Adjoint shape optimization applied to electromagnetic design. *Opt. Express* **2013**, *21*, 21693−21701.
(14) Shen, B.; Wang, P.; Polson, R.; Menon, R. An integrated-nanophotonics polarization beamsplitter with 2.4 × 2.4 μm2 footprint. *Nat. Photonics* **2015**, *9*, 378−382.
(15) Johnson, E. G.; Abushagur, M. A. G. Microgenetic-algorithm optimization methods applied to dielectric gratings. *J. Opt. Soc. Am. A* **1995**, *12*, 1152−1160.
(16) Preble, S.; Lipson, M.; Lipson, H. Two-dimensional photonic crystals designed by evolutionary algorithms. *Appl. Phys. Lett.* **2005**, *86*, 061111.
(17) Shokooh-Saremi, M.; Magnusson, R. Particle swarm optimization and its application to the design of diffraction grating filters. *Opt. Lett.* **2007**, *32*, 894−896.
(18) Forestiere, C.; Donelli, M.; Walsh, G. F.; Zeni, E.; Miano, G.; Dal Negro, L. Particle-swarm optimization of broadband nano-plasmonic arrays. *Opt. Lett.* **2010**, *35*, 133−135.
(19) Sell, D.; Yang, J.; Doshay, S.; Zhang, K.; Fan, J. A. Visible Light Metasurfaces Based on Single-Crystal Silicon. *ACS Photonics* **2016**, *3*, 1919−1925.
(20) Huntington, M. D.; Lauhon, L. J.; Odom, T. W. Subwavelength Lattice Optics by Evolutionary Design. *Nano Lett.* **2014**, *14*, 7195−7200.
(21) Wiecha, P. R.; Arbouet, A.; Girard, C.; Lecestre, A.; Larrieu, G.; Paillard, V. Evolutionary multi-objective optimization of colour pixels based on dielectric nanoantennas. *Nat. Nanotechnol.* **2016**, *12*, 163−169.
(22) Borel, P. I.; Harpøth, A.; Frandsen, L. H.; Kristensen, M.; Shi, P.; Jensen, J. S.; Sigmund, O. Topology optimization and fabrication of photonic crystal structures. *Opt. Express* **2004**, *12*, 1996−2001.
(23) Jensen, J. S.; Sigmund, O. Topology optimization for nano-photonics. *Laser Photonics Rev.* **2011**, *5*, 308−321.
(24) Piggott, A. Y.; Lu, J.; Lagoudakis, K. G.; Petykiewicz, J.; Babinec, T. M.; Vučković, J. Inverse design and demonstration of a compact and broadband on-chip wavelength demultiplexer. *Nat. Photonics* **2015**, *9*, 374−377.
(25) Lin, Z.; Pick, A.; Lončar, M.; Rodriguez, A. W. Enhanced Spontaneous Emission at Third-Order Dirac Exceptional Points in Inverse-Designed Photonic Crystals. *Phys. Rev. Lett.* **2016**, *117*, 107402.
(26) Fu, S. M.; Zhong, Y. K.; Ju, N. P.; Tu, M. H.; Chen, B. R.; Lin, A. Broadband Polarization-Insensitive Metamaterial Perfect Absorbers Using Topology Optimization. *IEEE Photonics J.* **2016**, *8*, 1−11.
(27) Sheng, X.; Johnson, S. G.; Michel, J.; Kimerling, L. C. Optimization-based design of surface textures for thin-film Si solar cells. *Opt. Express* **2011**, *19*, A841−A850.
(28) Xiao, T. P.; Cifci, O. S.; Bhargava, S.; Chen, H.; Gissibl, T.; Zhou, W.; Giessen, H.; Toussaint, K. C.; Yablonovitch, E.; Braun, P. V. Diffractive Spectral-Splitting Optical Element Designed by Adjoint-Based Electromagnetic Optimization and Fabricated by Femtosecond 3D Direct Laser Writing. *ACS Photonics* **2016**, *3*, 886−894.
(29) Botten, I. C.; Craig, M. S.; McPhedran, R. C.; Adams, J. L.; Andrewartha, J. R. The Dielectric Lamellar Diffraction Grating. *Opt. Acta* **1981**, *28*, 413−428.
(30) Lalanne, P.; Hugonin, J. P.; Chavel, P. Optical Properties of Deep Lamellar Gratings: A Coupled Bloch-Mode Insight. *J. Lightwave Technol.* **2006**, *24*, 2442.

DOI: 10.1021/acs.nanolett.7b01082
Nano Lett. 2017, 17, 3752−3757

(31) Hugonin, J. P.; Lalanne, P. *Reticolo software for grating analysis*; Institut d'Optique: Orsay, France, 2005.
(32) Wang, F.; Jensen, J. S.; Sigmund, O. Robust topology optimization of photonic crystal waveguides with tailored dispersion properties. *J. Opt. Soc. Am. B* **2011**, *28*, 387−397.

DOI: 10.1021/acs.nanolett.7b01082
Nano Lett. 2017, 17, 3752−3757